

Mystery of resonances in heavier systems

Eiji Uegaki

Graduate School of Engineering and Resource Science, Akita University,
Akita 010-8502, Japan

E-mail: uegaki@phys.akita-u.ac.jp

Abstract. Studies of resonances in heavier systems are reviewed. A molecular model developed for heavy-ion resonances is described briefly. At high spins, stable dinuclear configurations are obtained as an equator-equator touching one for $^{28}\text{Si} + ^{28}\text{Si}$ (oblate-oblate system) and a pole-to-pole one for $^{24}\text{Mg} + ^{24}\text{Mg}$ (prolate-prolate system), respectively. Normal modes have been investigated around those equilibria. Those modes are expected to be the origin of a large number of the resonances observed. Furthermore, it is clarified that those different-type of equilibria give rise to their own characteristic rotational excitations. The importance of recent experimental data measured in Strasbourg, for both the $^{28}\text{Si} + ^{28}\text{Si}$ and the $^{24}\text{Mg} + ^{24}\text{Mg}$ systems are stressed. Analyses of physical quantities are made and compared with those data.

1. Introduction

The $^{28}\text{Si} + ^{28}\text{Si}$ and $^{24}\text{Mg} + ^{24}\text{Mg}$ systems exhibit a number of narrow and prominent resonances well above the Coulomb barrier, which are correlated among the elastic and inelastic channels [1, 2]. Maximum spins of both resonance systems are close to or over $40\hbar$, and the mass-asymmetric decays are much smaller than symmetric ones. In addition, high level densities over ‘one per MeV’ are observed. Those observations suggest rather long-lived compound systems in an extreme condition, but their structures as well as reaction mechanism are not known yet. Thus they remain a complete mystery. This is quite in contrast with lighter systems explained by the double resonance mechanism, such as band crossing model [3].

From the consideration of dinuclear structures with well-deformed constituent nuclei, the author and Y Abe proposed a new molecular model, in which internal degrees of freedom are introduced with the orientations of the deformation axes of the constituent nuclei. We investigated normal modes of motion at the equilibrium dinuclear configurations for high spins, which gave rise to various excitation modes such as butterfly and antibutterfly ones, and would be responsible for a large number of resonances observed [4, 5, 6, 7]. The analyses with a method of normal mode are briefly described in section 2.

The two systems exhibit rather different features. Namely, the $^{28}\text{Si} + ^{28}\text{Si}$ system shows a large number of sharp peaks on the bumps associated with the grazing angular momenta [8, 9], while the $^{24}\text{Mg} + ^{24}\text{Mg}$ system shows several prominent and isolated peaks [2]. Recently two important issues have appeared from Strasbourg. For $^{28}\text{Si} + ^{28}\text{Si}$ at $E_{\text{cm}} = 55.8$ MeV, the angular distributions exhibit disalignments between the orbital angular momentum and the fragment spins, and the particle- γ angular correlation measurements show characteristic features [10]. The other is the $^{24}\text{Mg} + ^{24}\text{Mg}$ experiment, which shows the important role of the $(4^+, 4^+)$ channel as well as the single and mutual 2^+ channels [11]. The analyses for those experimental



data are given, for the $^{28}\text{Si} + ^{28}\text{Si}$ system in section 2 and for the $^{24}\text{Mg} + ^{24}\text{Mg}$ system in section 3, which clarify characteristic features of those systems.

2. Dinuclear molecular model for the $^{28}\text{Si} + ^{28}\text{Si}$ system

2.1. Stable molecular configurations at high spins

In fig. 1, stable molecular configurations at high spins are displayed, where the upper one is for $^{24}\text{Mg} - ^{24}\text{Mg}$ and the lower one for the $^{28}\text{Si} - ^{28}\text{Si}$ system. Those equilibria are obtained by the molecular model, which will be explained later in this section. Because of centrifugal energy dominance, such elongated configurations appear with relatively lower energy, with contacts at the tips of the constituent nuclei. Normal mode analyses have been made around those equilibrium configurations with four internal degrees of freedom.

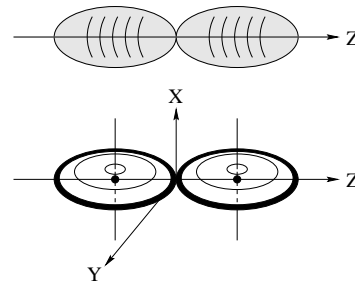


Figure 1. Equilibrium configurations of two dinuclear systems, $^{24}\text{Mg} - ^{24}\text{Mg}$ and $^{28}\text{Si} - ^{28}\text{Si}$.

2.2. Degrees of freedom and normal modes

For simplicity, assuming a constant deformation and an axial symmetry of the constituent nuclei, we have seven degrees of freedom, $(q_i) = (\theta_1, \theta_2, \theta_3, R, \alpha, \beta_1, \beta_2)$ illustrated in fig. 2, where (R, θ_2, θ_1) is the relative vector of the two ^{28}Si nuclei. As internal degrees of freedom, the orientations of the symmetry axes of the two constituent ^{28}Si nuclei are described with the Euler angles (α_i, β_i) , which refer to the molecular axes. α_1 and α_2 are combined into $\theta_3 = (\alpha_1 + \alpha_2)/2$ and $\alpha = (\alpha_1 - \alpha_2)/2$.

The kinetic energy is given classically in terms of angular velocities, and then the quantization is done to describe the rotation of the whole system with the total angular momentum operator \hat{J} and the internal motions referring to the molecular axes. The nucleus-nucleus interaction is given with folding potential using the nucleon-nucleon interaction DDM3Y. Expecting a stable configuration, the interaction potential is described with geometrical configurations specified by the internal degrees $(R, \alpha, \beta_1, \beta_2)$. Consistently with the coordinate system, at first we introduce a rotation-vibration type wave function as basis one, $\Psi_\lambda \sim D_{MK}^J(\theta_i)\chi_K(R, \alpha, \beta_1, \beta_2)$, where χ_K describes the internal motions. In fig. 3, a multidimensional energy surface including centrifugal energies is displayed. A local minimum is obtained around $\beta = 90^\circ$ and $R = 7.6$ fm with the

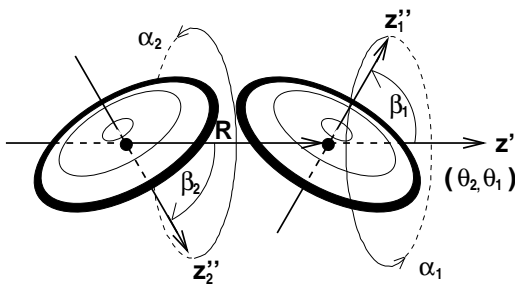


Figure 2. Dinuclear molecular coordinates; seven degrees of freedom of the $^{28}\text{Si} + ^{28}\text{Si}$ system are displayed,

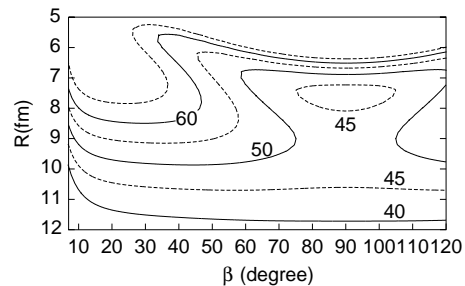


Figure 3. Contours of the effective potential energy V_{JK} with $J = 38$ and $K = 0$ for the $R - \beta(\beta_1 = \beta_2)$ degrees at $\alpha = \pi/2$.

barrier at ~ 9.5 fm, which is an *equator-equator* (E-E) configuration illustrated in the lower portion of fig. 1.

In order to solve the internal motions, we expand the effective potential at the energy minimum point and adopt the harmonic approximation to obtain the normal modes. Motions associated with β degrees are well confined to be vibrational, which are classified into new modes, *butterfly*: $\beta_+ = (\Delta\beta_1 + \Delta\beta_2)/\sqrt{2}$ and *antibutterfly*: $\beta_- = (\Delta\beta_1 - \Delta\beta_2)/\sqrt{2}$ around $\alpha = \pi/2$, respectively. In fig. 4(a) molecular normal modes of $^{28}\text{Si} + ^{28}\text{Si}$ with spin 38 are displayed, classified with quantum numbers K . Butterfly and antibutterfly modes are indicated with (b) under the levels. As for the α degree, $\alpha = (\alpha_1 - \alpha_2)/2$, the confinements in the present folding potential appear to be unexpectedly weak, and hence the motion is close to a free rotation. We call it *twisting mode*, the associated levels of which are indicated by (t). All those are due to internal degrees of freedom, i.e., intrinsic excitations. These excitations exist over the range of spin $J = 34 - 40$ in which the E-E configuration is stable, and are expected to be the origin of the narrow resonances.

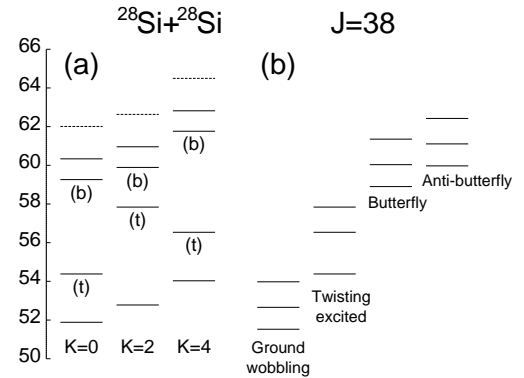


Figure 4. Energy spectra of the $^{28}\text{Si} + ^{28}\text{Si}$ system for $J = 38$. (a) Molecular normal modes without K -mixing. (b) After K -mixing, with indication of the modes under the levels.

2.3. Wobbling motion with triaxial deformation

One of the characteristic features of the molecular spectrum is a series of low-energy K rotational excitation due to axial asymmetry around molecular z' axis, which is in contrast with the $^{24}\text{Mg} + ^{24}\text{Mg}$ case [4]. One can understand the reason immediately from fig. 1, where the upper configuration ($^{24}\text{Mg} + ^{24}\text{Mg}$) has axial symmetry as a total system, but the lower one for $^{28}\text{Si} + ^{28}\text{Si}$ has axial asymmetry. Thus K is not a good quantum number, namely, we expect that the eigenstates are K -mixed. In general, a triaxial system preferentially rotates around the axis with the largest moment of inertia. The oblate-oblate system, which can be seen as two pancake-like objects touching side-by-side in the lower panel of fig. 1, rotates around the X axis which is parallel to the normal to the reaction plane.

Those motions at high spins due to axial asymmetry give rise to mixing of quantum numbers K , which is known as *wobbling*. In the high spin limit ($K/J \sim 0$), the diagonalization in the K space is found to be equivalent to solving of the differential equation of the harmonic oscillator with parameters given by the moments of inertia. Thereby, the solution is a Gaussian, or a Gaussian multiplied by an Hermite polynomial, $F_n(K) = H_n(K/b) \exp[-(K/b)^2/2]$, with the width b given by the asymmetry of the moments of inertia. For the wobbling ground state, the total wave function is given with $F_0(K)$ as

$$\Psi_\lambda^{JM} \sim \sum_K \exp(-K^2/2b^2) D_{MK}^J(\theta_i) \chi_K(R, \alpha, \beta_1, \beta_2), \quad (1)$$

where in general, χ_K can be any molecular mode of triaxial deformations, such as the ground-state configuration or the butterfly modes. The resultant energy spectrum is displayed in fig.4(b) and compared with the spectrum without K -mixing in fig. 4(a).

In the experimental angle-averaged excitation functions, bumps are seen corresponding to the grazing angular momenta, the values of which are suggested by the Legendre fits [8]. Several sharp peaks are found on each bump [9], and thus those excited states with $J = 38$ are expected to the origin of those sharp peaks.

2.4. *Disalignments: observed $L = J$ dominance*

In the $^{28}\text{Si} + ^{28}\text{Si}$ system at 55.8 MeV, disalignments between the orbital angular momentum L and the fragment spins have appeared as a novel aspect of heavy-ion resonances [10], which has never been observed in any heavy-ion system so far and is considered mysterious.

Our molecular model naturally explains the mechanism of those disalignments, as is illustrated in fig. 5. Due to the characteristic rotational motion preferentially around the X axis, i.e., *wobbling*, the spins of the ^{28}Si fragments are approximately in the reaction plane, because they are in the YZ plane, as they are perpendicular to the symmetry axes of the constituent ^{28}Si nuclei. Thus the disalignments observed in the angular distributions, i.e., $L = J$ oscillation patterns both in the single and mutual 2^+ channels are well reproduced by the analyses with R -matrix theory [7].

2.5. *Angular-correlation measurements: ‘ $m=0$ ’ characteristics*

Furthermore, fragment-fragment- γ angular correlations have been measured, which show a characteristic ‘ $m = 0$ ’ pattern of the γ distribution, and thus we have analyzed those data. Dots in fig. 6 display the angular correlation data [10], i.e., γ -ray intensity distributions of the $E2$ transition observed in the mutual 2^+ channel, and solid lines show theoretical results of the molecular ground state. Three different quantization axes are taken in panels (a)–(c), respectively: (a) beam direction, (b) z axis normal to the scattering plane, and (c) z axis perpendicular to those of (a) and (b). In panel (b) a typical ‘ $m = 0$ ’ pattern is obtained, and the results show good agreements in all the three panels. Again, figure 5 explains the origin of ‘ $m = 0$ ’, which means not only that the spins are in the reaction plane, but also that the spins in the Y and Z directions are almost the same in their strengths. Thus, the stable E-E configuration with the axial asymmetry rotates wobblingly around the axis normal to the reaction plane, which gives rise to the ‘ $m = 0$ ’ dominance [7].

In the angular correlations of the twisting excitation and the butterfly modes, clear differences from the molecular ground state are seen. For example, dashed lines in fig. 6 display the results of the twisting excitation, where a ‘ $m = 1$ ’ pattern appears in (b). The essential feature of the twisting excitation is ‘ $m = 2$ ’ dominance in panel (a), where the z axis is parallel to the beam direction. This means that the spin directions are not in B, but in A of fig. 5, due to the twisting motion around the molecular z' axis [7]. Such characteristics are also seen in the high excitation of the wobbling motion, where two ^{28}Si nuclei rotate around the molecular z' axis [12]. Thus the normal modes have their own characteristics in angular correlations, which give identifications of the normal-mode excitations, i.e. of the intrinsic nuclear structure of the resonances.

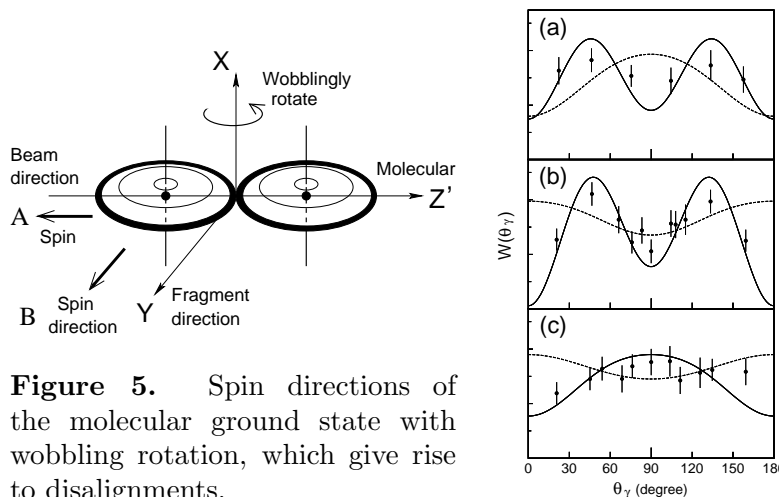


Figure 5. Spin directions of the molecular ground state with wobbling rotation, which give rise to disalignments.

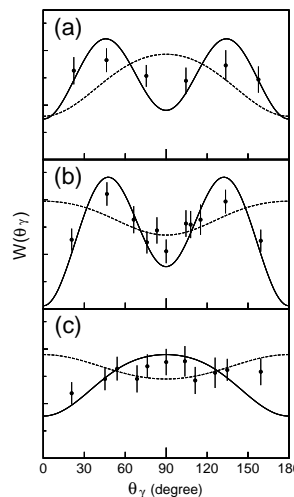


Figure 6. γ -ray intensities of particle-particle- γ angular correlations in the mutual 2^+ channel. Dots display the experimental data [10]. Solid lines show theoretical results of the molecular ground state, and dashed lines show those of the twisting rotational state. See text for the quantization axes of three panels.

3. Normal-mode spectrum for butterfly and antibutterfly; How they appear in the resonances of the $^{24}\text{Mg} + ^{24}\text{Mg}$ system?

3.1. Recent progress in the experimental study

Narrow and prominent resonance peaks are observed by Zurmühle *et al* in the $^{24}\text{Mg} + ^{24}\text{Mg}$ system around $E_{\text{cm}} = 46$ MeV, and four peaks starting from 45.7 MeV are assigned to be $J = 36$ [2]. We have analyzed the probability distributions in the decay channels and the partial widths for the normal mode excitations of the $^{24}\text{Mg} + ^{24}\text{Mg}$ system, and have showed that the excitation brings enhancements in the higher spin channels, such as 4^+ ones [13]. Recently, Salsac and Haas *et al* have made an experiment at $E_{\text{cm}} = 45.7$ MeV [11]. They showed that the 4^+ channels take much larger contributions to the resonance than those of the 2^+ channels, which is in good agreement with our analyses. In addition, they showed that the contribution from the 6^+ channel is quite small. Such a feature is seen in the angle averaged yields of Zurmühle *et al*, where strong $(4^+, 4^+)$ channel decays are observed [2]. Interesting is that enhancements of the $(4^+, 4^+)$ channel are seen to be rather different from those of the single and mutual 2^+ channels about excitation energies. Note that in the figure of Zurmühle's paper, the $(4^+, 4^+)$ channel is indicated as 6^+ , since it is not possible to divide their contributions.

Now it is necessary to pay much attention to the mutual 4^+ channel. In table 1 data of the partial widths up to the $(4^+, 4^+)$ channel are collected [14] for the resonances at $E_{\text{cm}} = 45.66, 46.64$ and 47.25 MeV. In the resonance at 45.66 MeV, the contribution of the $(4^+, 4^+)$ channel is much larger than that of the $(2^+, 2^+)$ channel, while it is very small in the 46.64 MeV resonance, which suggests that the properties of those states are different.

Table 1. Partial widths (ratio $\Gamma_{\text{channel}}/\Gamma$ in percent) of the resonances at $E_{\text{cm}} = 45.66, 46.64$ and 47.25 MeV observed in the elastic and inelastic scattering of $^{24}\text{Mg} + ^{24}\text{Mg}$ [14].

$E_{\text{R}}(\text{MeV})$	$\Gamma(\text{keV})$	Final state:						
		g.s.	2^+0^+	2^+2^+	4^+0^+	4^+2^+	4^+4^+	
45.66	180 ± 25	1.75	3.80	4.40	2.10	2.15	11.00	
46.64	230 ± 30	1.47	7.40	5.10	2.10	3.50	2.80	
47.25	195 ± 30	1.39	4.90	2.70	0.65	1.10	5.40	

3.2. Normal-mode analysis of the $^{24}\text{Mg} + ^{24}\text{Mg}$ system

In the $^{24}\text{Mg} + ^{24}\text{Mg}$ system the normal-mode energy spectrum is rather different from the $^{28}\text{Si} + ^{28}\text{Si}$ case. We can understand the basic aspect of the excitation in the pole motion from the equilibrium configuration of the $^{24}\text{Mg} + ^{24}\text{Mg}$ system, in which two pole tips are touching, as is seen in the upper panel of fig. 1. The vibrational motions of poles are available around the Z axis, both to the X and Y directions, which means that the dynamics of the single pole motion basically follows that of a two-dimensional harmonic oscillator. In addition, with two poles of prolate-deformed nuclei, their coupling should be taken into account. Thus we solved the single pole motion first, and then diagonalized the coupling between the two poles, with respect to the $(\alpha, \beta_1, \beta_2)$ degrees of freedom. In fig. 7, the normal-mode spectrum is displayed, where the levels displayed with short widths are those of the basic spectrum obtained at the first step. The levels C have two $\hbar\omega_\beta$ for the butterfly excitations with $K = 0$, while the level B exhibits radial excitation. Due to the interaction energy difference between the butterfly and antibutterfly motions, which are illustrated in fig. 8, the degenerate levels split: for example, the levels C separate into two, about 2 MeV apart. The other levels D to L are also dissolved by such an interaction, which gives rise to the normal mode spectrum [4].

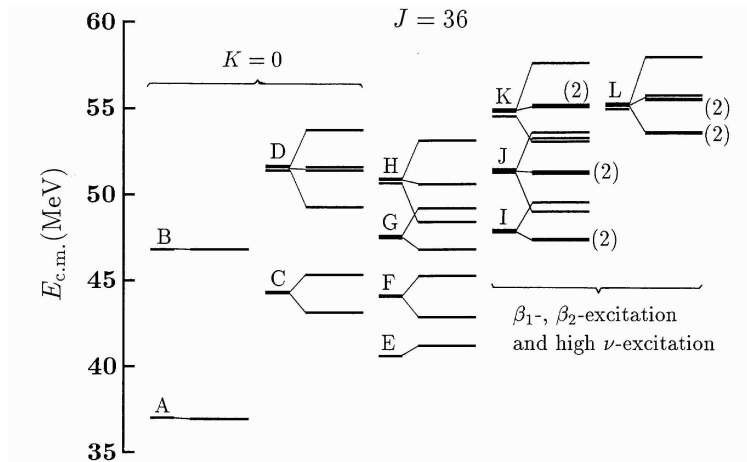


Figure 7. Energy spectra for the normal modes of the $^{24}\text{Mg} + ^{24}\text{Mg}$ system with $J = 36$ [4]. Levels displayed with short widths on the *l.h.s.* show the basic spectrum obtained without the orientation coupling between two poles. Level B shows the radial excitation. Levels A to D are of $K = 0$, and levels from E to H display $K = 1$ to $K = 4$ states, respectively. The degenerate levels of C split into two, i.e., butterfly and antibutterfly levels due to the interaction between pole tips.

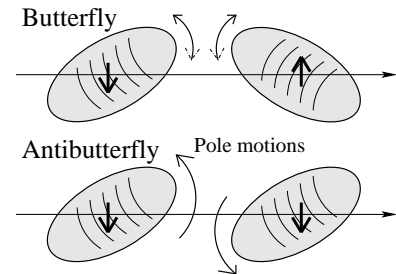


Figure 8. Illustrations of configurations for the butterfly mode (upper portion) and the antibutterfly mode (lower one), where the motions of poles of the ^{24}Mg nuclei are indicated by round allows. Bold arrows at the center of the ^{24}Mg nuclei show spin directions expected from those motions of the poles, respectively.

The physical properties of the butterfly modes have been investigated by the analyses of the partial widths. In fig. 9, probability distributions on the channel spins I are displayed for the $(4^+, 2^+)$ channel of the $^{24}\text{Mg} + ^{24}\text{Mg}$ system and the $(2^+, 2^+)$ channel of the $^{28}\text{Si} + ^{28}\text{Si}$ system, which are the dominant channels in the butterfly excitations. Characteristic features are seen for the dominant channel spins I in the two butterfly-type modes, i.e., $I \sim$ ‘minimum’ in butterfly, while $I \sim$ ‘maximum’ in antibutterfly [13]. We can easily understand such a mechanism of each mode from the spin directions caused by the butterfly motion, as is illustrated in fig. 8. Correspondingly to the channel spins, the dominant decay channels appear with quite different characteristics. In the antibutterfly state, the largest decay yield appears in the $(4^+, 2^+)$ channel, as expected. However, in the butterfly state the largest yield does not appear in the $(4^+, 2^+)$ channel, but appears in the $(2^+, 2^+)$ channel. This is due to dominant decaying angular momentum

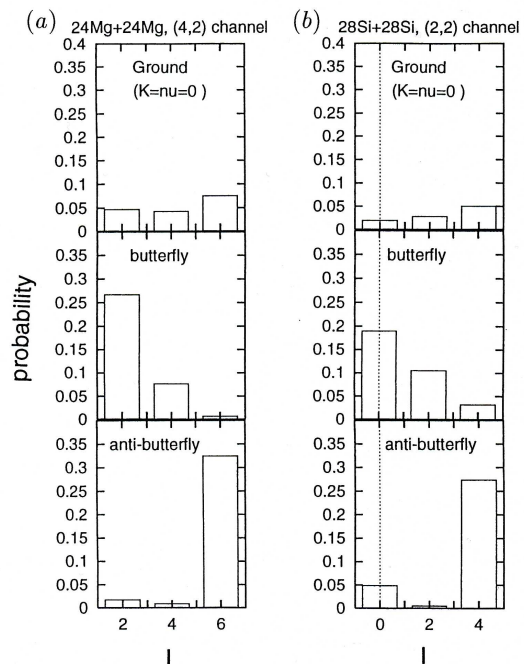


Figure 9. Probabilities in the channel spin I , for the systems (a) $^{24}\text{Mg} + ^{24}\text{Mg}$ with $J = 36$ and (b) $^{28}\text{Si} + ^{28}\text{Si}$ with $J = 38$, respectively.

values L , which are $L \sim 30$ with alignments of L and I in the former, while $L \sim 36$ with the small I value in the latter. The observation of the strong or weak enhancements of the $(4^+, 4^+)$ channel for each resonance at 45.66 MeV or 46.64 MeV discussed in section 3.1, are expected to correspond to such a mechanism.

4. Conclusions

Studies for resonances in heavier systems have been reviewed. By using a molecular model, the interaction between two deformed nuclei is described with the internal collective variables. Molecular normal modes have been obtained, such as butterfly and antibutterfly ones in addition to the radial excitation, which give rise to a variety of molecular states. Those modes are expected to be the origin of a large number of the resonance states.

For the $^{28}\text{Si} - ^{28}\text{Si}$ resonance states the results show that the structure is an asymmetrically hyperdeformed molecule [5, 6]. By the R -matrix theory, analyses of the decay properties have been made [7]. Each normal mode exhibits its own different characteristics in the angular correlations. In other words, the angular correlation measurements provide information to distinguish among molecular intrinsic states of the resonances. Due to the axial asymmetry of the stable configuration, the system rotates wobblingly around the axis normal to the reaction plane, which gives rise to the ' $m = 0$ ' dominance in the molecular ground state and good agreement with the experiment on the $E_{\text{cm}} = 55.8$ MeV resonance.

For the $^{24}\text{Mg} + ^{24}\text{Mg}$ system, in the analysis on the partial widths [13] it is found that the butterfly mode has a small channel-spin value, while the antibutterfly mode has a large value. This mechanism is expected to give rise to disalignments and alignments, respectively.

With respect to the mutual 4^+ channel, its importance has been ignored, even though the contributions from this channel are very large. However, since Salsac and Haas have shown the importance of the 4^+ channels [11], the first data by Zurmühle *et al* [2] are reviewed. The statistical analyses exhibit strong or weak enhancements in the mutual 4^+ channel at different resonance energies [14]. Thus the above mechanism suggested theoretically is in agreement with the experimental data at present, and has to be confirmed by a further study.

As a whole, resonances in the heavier systems provide new, intriguing knowledge on nuclear structure and dynamics. The experimental challenges to uncover the characteristic features of the resonances are strongly desired.

Acknowledgments

The author heartily thanks to Dr Y Abe, for many discussions and encouragements in the collaboration for resonances in heavier systems.

References

- [1] Betts R R 1985 *Clustering Aspects of Nuclear Structure* (Dordrecht: D Reidel) p 133
- [2] Zurmühle R W, Kutt P, Betts R R, Saini S, Haas F and Hansen Ole 1983 *Phys. Lett.* **129B** 384
- [3] Abe Y, Kondō Y and Matsuse T 1980 *Prog. Theor. Phys. Suppl. No.* **68** 303
- [4] Uegaki E and Abe Y 1993 *Prog. Theor. Phys.* **90** 615
- [5] Uegaki E and Abe Y 1994 *Phys. Lett. B* **340** 143
- [6] Uegaki E and Abe Y 2012 *Prog. Theor. Phys.* **127** 831
- [7] Uegaki E and Abe Y 2012 *Prog. Theor. Phys.* **127** 877
- [8] Betts R R, DiCenzo S B and Petersen J F 1981 *Phys. Lett.* **100B** 117
- [9] Betts R R, Back B B and Glagola B G 1981 *Phys. Rev. Lett.* **47** 23
- [10] Nouicer R *et al* 1999 *Phys. Rev. C* **60** 041303
- [11] Salsac M-D *et al* 2008 *Nucl. Phys. A* **801** 1
- [12] Uegaki E and Abe Y 2013 *Proc. of this conference*
- [13] Uegaki E 1998 *Prog. Theor. Phys. Suppl. No.* **132** 135
- [14] Saini S, Betts R R, Zurmühle R W, Kutt P H and Dichter B K 1987 *Phys. Lett. B* **185** 316